Nanoscale Advances

ROYAL SOCIETY OF CHEMISTRY

PAPER

View Article Online
View Journal | View Issue

Cite this: *Nanoscale Adv.*, 2020, **2**, 3411

Echogenic exosomes as ultrasound contrast agents

Jenna Osborn,†[a] Jessica E. Pullan,†[b] James Froberg,[c] Jacob Shreffler,[b] Kara N. Gange,[d] Todd Molden,[e] Yongki Choi,[c] Amanda Brooks,[b] Sanku Mallik[b] and Kausik Sarkar*[a]

Exosomes are naturally secreted extracellular bilayer vesicles (diameter 40–130 nm), which have recently been found to play a critical role in cell-to-cell communication and biomolecule delivery. Their unique characteristics—stability, permeability, biocompatibility and low immunogenicity—have made them a prime candidate for use in delivering cancer therapeutics and other natural products. Here we present the first ever report of echogenic exosomes, which combine the benefits of the acoustic responsiveness of traditional microbubbles with the non-immunogenic and small-size morphology of exosomes. Microbubbles, although effective as ultrasound contrast agents, are restricted to intravascular usage due to their large size. In the current study, we have rendered bovine milk-derived exosomes echogenic by freeze drying them in the presence of mannitol. Ultrasound imaging and direct measurement of linear and nonlinear scattered responses were used to investigate the echogenicity and stability of the prepared exosomes. A commercial scanner registered enhancement (28.9% at 40 MHz) in the brightness of ultrasound images in presence of echogenic exosomes at 5 mg mL^{-1}. The exosomes also showed significant linear and nonlinear scattered responses—11 dB enhancement in fundamental, 8.5 dB in subharmonic and 3.5 dB in second harmonic all at 40 μg mL^{-1} concentration. Echogenic exosomes injected into the tail vein of mice and the synovial fluid of rats resulted in significantly higher brightness—as much as 300%—of the ultrasound images, showing their promise in a variety of *in vivo* applications. The echogenic exosomes, with their large-scale extractability from bovine milk, lack of toxicity and minimal immunogenic response, successfully served as ultrasound contrast agents in this study and offer an exciting possibility to act as an effective ultrasound responsive drug delivery system.

Received 28th April 2020
Accepted 15th June 2020

DOI: 10.1039/d0na00339e

rsc.li/nanoscale-advances

1. Introduction

The role of exosomes as a tool in research and clinical applications continues to grow. An increasing number of new research articles are being published using exosomes in various unique facets of biomedical research, including drug delivery and diagnostics. Exosomes are ubiquitous, secreted, membrane-derived vesicles that play a critical role in cellular communication through the transportation of biological macromolecules, such as RNA and proteins.[1] Ranging from 40 to 130 nm in diameter, exosomes have the same lipid bilayer composition as the excreting cell, including the extracellular proteins and polysaccharides.[1,2] Internal contents of exosomes also vary depending on secreting host cell signals. Unfortunately, much remains unknown about the cellular mechanisms prompting and determining the exosome's encapsulation contents. Recently, exosomes have gained attention not only for their small size and natural, cell-like morphology but also for being universally present in bodily fluids regardless of species.[1] Although it is tempting to equate exosomes with nanoparticles due to their small size and ability to transport contents, the ability of exosomes to interact with cell membranes without eliciting an immune response is a distinct advantage.[1] The innate ability of exosomes to circumvent many of the natural immune system clearance pathways, due to their cell-like properties, may overcome one of the greatest barriers to the clinical translation of nanoparticles.

Due to their unique physical features, exosomes are becoming prevalent as a drug delivery tool in preclinical research and clinical trials for both cancer and arthritis. The ability for exosomes to transport hydrophobic, hydrophilic and large biomolecules allows a broad spectrum of treatment (*e.g.*, genetic materials, proteins or small molecules) to quickly reach a desired tissue.[3] While most previous efforts have focused on the utility of exosomes in drug delivery, they also hold great potential for diagnostics as well.[3] The ability to treat complex pathologies is rapidly expanding and revealing not only the

[a]*Mechanical and Aerospace Engineering, George Washington University, Washington DC 20052, USA. E-mail: sarkar@gwu.edu*
[b]*Pharmaceutical Sciences, North Dakota State University, Fargo, ND 58105, USA*
[c]*Physics, North Dakota State University, Fargo, ND 58105, USA*
[d]*Health, Nutrition, and Exercise Science, North Dakota State University, Fargo, ND 58105, USA*
[e]*Animal Science, North Dakota State University, Fargo, ND 58105, USA*
† Authors have contributed equally to the work.

importance of early disease diagnosis but also a gap in the available tools to do so. Exosomes may fill that gap, having the ability to detect either through molecular and/or visual recognition. While patient derived exosomes are no longer thought to be a viable delivery strategy due to incomplete characterization of their transported cargo, which may potentially confer pathology, bovine and healthy cell culture derived exosomes are becoming more popular. The same reasons that argue against using patient derived exosomes for drug delivery, make them excellent for diagnostics. Exosome cargo can be analyzed to examine specific markers for disease states leading to faster and earlier diagnosis.[4–6] Identification of disease state biomarkers combined with the exosomes ability to carry a defined cargo, may bridge the gap between delivery and diagnostics.

Despite intense efforts in nanoparticle enabled biomedical research,[7,8] clinical translation of nanoparticles has lagged behind, leaving their promise largely unfulfilled.[9] Nevertheless, many lessons can be learned from both their successes and failures. Nanoparticles – particles with diameters less than 200 nm – have gained attention for their ability to enhance the delivery of drugs with active or passive targeting mechanisms.[1,10] The nanoparticles' ability to target tissues and effectively deliver drugs has been successful in preclinical trials, specifically those in cancer therapy.[3,11–14] While surprisingly few of these nanoparticle drug delivery studies have transitioned to broad clinical adoptions, nanoparticles have been more successful as a diagnostic/visualization tool, with their prevalence continuing to increase.[15,16] Previously, we have performed detailed acoustic characterizations of echogenic nanoparticles (*i.e.*, liposomes and polymersomes) by varying their properties and shell chemistry.[17–21] Tracing diagnostic nanoparticles has revealed rapid nanoparticle clearance rates and adverse immune responses as the point of failure for many clinical trials.[22] However, unlike synthetic nanoparticles, many exosomes do not face these same issues potentially making them a more viable option for clinical drug delivery and diagnostics.[3,23] Combining the advantages of naturally derived exosomes to make the particle echogenic is a particularly exciting approach to demonstrate the utility of exosomes in biomedical research.[17,18,24–27]

Ultrasound is known as a safe, inexpensive, and real-time imaging modality. However, it suffers from low contrast.[28,29] The low contrast is alleviated with the addition of intravenously injectable microbubble-based ultrasound contrast agents (UCA).[30] The Food and Drug Administration (FDA) approved their use in echocardiography as a diagnostic tool for myocardial microperfusion in 2001 and in liver imaging in 2016.[31–33] The UCAs range between 1–5 μm in diameter and have a lipid, polymer, or protein shell with a perfluorocarbon gas core for enhanced stability.[34–36] Due to the compressible nature of the gas core, UCAs oscillate under ultrasound excitation generating linear and nonlinear (sub- and higher harmonic) responses that can improve the enhancement of ultrasound image contrast.[37–41] UCA oscillations also cause acoustic microstreaming flows surrounding the microbubble leading to enhanced mixing and shear stress experienced by nearby cell membranes.[31,42] The shear stress is believed to increase membrane permeability or excite mechanosensitive ion channels, potentially allowing for therapeutic drug delivery to the cells.[43,44] However, UCAs are restricted to the vascular system as they are too large to permeate outside of the blood vessels. For extravascular imaging and ultrasound medicated therapeutic applications, researchers have sought smaller, nanosized echogenic particles.[45,46] Here, we report a first ever study of exosomes, made echogenic, for imaging applications.

To quantify and understand the acoustic behaviors of the engineered, echogenic exosomes, their echogenicity was investigated by directly measuring their linear and nonlinear scatter responses in a customized *in vitro* setup and by imaging with a commercial scanner *in vivo*. Overall, the ability to make exosomes ultrasound responsive shows excellent promise for contrast enhanced ultrasound imaging and concurrent drug delivery. In the current study, bovine milk derived exosomes, which offer the added advantages of large-scale production along with strong biocompatibility and minimal immunogenic response, were made echogenic. Our development of echogenic exosomes has potentials as a diagnostic and drug delivery separately and in combination.[47,48]

2. Experimental methods

2.1 Exosome isolation

Raw bovine milk was collected from the North Dakota State University Dairy Farm in 1 L quantities. If the raw bovine milk was not used the same day of pickup, it was stored at 4 °C for up to 4 days. Due to the fat content of the milk, serial centrifugation was used to isolate exosomes. Raw bovine milk was placed in six 50 mL centrifuge tubes with 45 mL in each and spun for 20 min a 3500*g* in a VWR Clinical 200 Centrifuge. Following the initial 20 minute spin, white fat deposits formed on the wall of the centrifuge tubes and the milk was passed through a cheesecloth to remove fat. A Beckman Coulter Optima LE-80K Ultracentrifuge was used with a 28 W rotor for the remainder of centrifugation steps. After being passed through the cheesecloth, the milk was collected and placed with equal weight into six 38.5 mL thin wall, Ultra-Clear tubes (Beckman Coulter, CA, USA.). Tubes were spun at 12 950*g* at 4 °C for 30 minutes. The milk was removed from the tubes and was filtered through cheesecloth to remove more fat. Once the milk was filtered, it was placed in 4 new ultracentrifuge tubes and spun at 98 500*g* for 70 minutes at 4 °C. Three layers then formed in each tube and the middle layer was collected. The middle layer was then placed in two fresh ultracentrifuge tubes and spun at 135 030*g* for 1 hour and 45 min at 4 °C. Subsequently, the liquid was removed from the ultracentrifuge tubes, taking care not to disturb the pellet. The pellet was then resuspended in 400 μL of phosphate buffer solution (1× Dulbecco's PBS, VWR). Both tubes of PBS suspended exosomes were combined leaving a clear film at the bottom of the tube. A 0.45 μm filter was prewet using PBS. Then the exosomes were passed through the filter into an Eppendorf tube. The first three drops of PBS in the syringe filter were discarded after the exosomes were filtered through using a 1 mL syringe using two separate filters. To ensure all exosomes were retrieved from the filter, more PBS was

passed through the filter until the first three drops come out and the remainder was discarded. Dynamic light scattering was performed to hydrodynamic diameters of the exosomes. Parafilm was placed around the outside of the Eppendorf tube and was kept at −80 °C until used.

2.2 Echogenic exosomes preparation

Exosomes were thawed at room temperature.[49] Once the exosomes reached room temperature, 210 μL of exosomes were added dropwise to 1.5 mL of 320 mM mannitol–HEPES buffer (pH 7.4) while stirring. After 10 minutes of stirring, pressurized filtered ambient air was bubbled in for 45 minutes. Following evaporation, the solution was sonicated for 60 minutes ensuring that the temperature does not exceed 30 °C. Sonication (Symphony Sonicator, 117 V, 60 Hz, VWR, USA) is a variable that was tested to determine its necessity in the protocol. Next, the sample was frozen in −80 °C for 1 day after which the sample was thawed in a 65 °C water bath. Three freeze–thaw cycles occurred each separated by 1 day. Following the freeze-thaw cycles, the sample was lyophilized for four days to prepare a powder.

2.3 Ultrasound imaging and processing

Echogenic exosomes were reconstituted in BSA–HEPES solution. The BSA–HEPES solution was made using 2.5 g of BSA in 500 mL of 10 mM HEPES buffer at pH 7.4. *In vitro* studies used a concentration of 5 mg mL^{-1} echogenic exosomes in BSA–HEPES. *In vivo* studies used 58 mg mL^{-1} and 150 mg mL^{-1} of echogenic exosomes. Vevo 3100 Imaging System (Fujifilm Visual Sonics, Toronto, ON, Canada) was used. Transducer heads with frequencies of 40 and 21 MHz were utilized for *in vitro*, and only 40 MHz was utilized for *in vivo* imaging. For frequencies 4–15 MHz, the ultrasound scan properties were set at high (H) frequency, level 51 2D Gain, level 60 Dynamic Range (DR), 3 cm scan depth, and 22 Hz frame rate using a 15L4 transducer head.

2.4 Atomic force microscopy (AFM)

The samples of echogenic exosomes were prepared by incubating 10 μL of each solution on silicon substrates (University Wafer) for 10 minutes in a sealed compartment to prevent evaporation at room temperature. The samples were then washed with de-ionized water (Millipore) and dried under purified nitrogen flow. The imaging measurements were performed using a commercial atomic force microscope (NT-MDT NTEGRA AFM). The samples were imaged under ambient conditions in semi-contact mode using an AFM tip with a resonant frequency of 190 kHz (Budget sensors).

2.5 Size and concentration

The dry powder of echogenic exosomes was reconstituted as 1 mg mL^{-1} for size distribution and concentration determination. All measurements were performed using qNano Gold with nanopore size NP150 (Izon Science™, Medford, MA). The sample size and concentration were calibrated during each measurement using the manufacturer's calibrations particles of carboxylated polystyrene beads (CPC100, average diameter: 110 nm, concentration: 1.1×10^{13} particles per mL). The samples were repeated at least 3 times on 3 different batches. Dynamic light scattering (DLS) was also performed on exosomes. The exosomes were isolated freshly for DLS. The samples were repeated at least 3 times on 3 different batches.

2.6 Western blot of exosomes

Exosomes were freshly isolated with storage at −80 °C for three days prior to lysing for analysis of exosomal membrane protein markers. These markers were assessed using ExoAb Antibody's CD63 and CD9 with their respective secondary antibodies (SBI System Biosciences, Palo Alto, CA) according to the manufacturer's protocol. Immuno-positive bands were detected using an ECL Plus kit (Invitrogen).

2.7 Linear and nonlinear acoustic characterization

A setup similar to what was used previously[17,24,50] was employed to characterize the acoustic scattering behavior of the echogenic exosomes (Fig. 1). Briefly, two spherically focused transducers positioned perpendicular to each other were confocally aligned in a 125 mL polycarbonate tank. The transmitting transducer had a center frequency of 5 MHz (Olympus, Waltham, MA, −6 dB bandwidth: 2.95–6.77 MHz, focal distance 1.2 in) with a pressure amplitude of 500 kPa, and receiving frequency of either 2.25 MHz (Olympus, Waltham, MA, −6 dB bandwidth 1.48–2.90 MHz, focal distance 1.2 in), 5 MHz (Olympus, Waltham, MA, −6 dB bandwidth: 2.95–6.77 MHz, focal distance 1.2 in), or 10 MHz (Olympus, Waltham, MA, −6 dB bandwidth 6.96–13.16 MHz, focal distance 1.2 in). All transducers were calibrated with a needle hydrophone (PZT-Z44-0400, Onda Corporation, CA, USA). A smaller, triangular 3D printed chamber of acrylonitrile butadiene styrene (ABS) with acoustically transparent windows was placed in the chamber, so the focus of the two transducers overlaps at the center of the chamber. The dry powder of the echogenic exosomes at a concentration of 40 μg mL^{-1} was reconstituted into either 10 mM HEPES buffer with or without 0.5% (w/v) BSA or only 0.5% (w/v) BSA. Then, 8 mL of

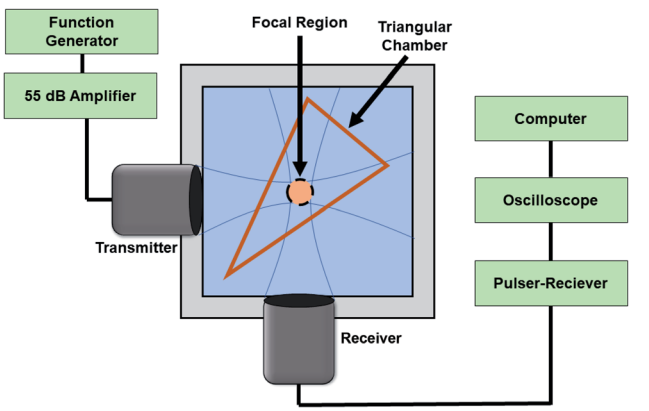

Fig. 1 The experimental setup for measuring the linear and nonlinear scattering response of the echogenic exosomes.

the reconstituted exosomes in respective solutions were placed inside the triangular chamber, and the surrounding volume was filled with deionized water. A function generator (Model AFG 3251, Tektronix, Beaverton, OR, USA) amplified by a 55 dB power amplifier (Model A-300; ENI, Rochester, NY, USA) excited the transmitting transducer to produce a 32-cycle sinusoidal pulse at 500 kPa amplitude, 5 MHz frequency and pulse repetition frequency of 100 Hz. The scattered response was obtained by a pulsar/receiver (Panametrics 5800, Waltham, MA, 6qUSA) with 20 dB gain through a receiving transducer. Signals were averaged over 64 sequences to improve the signal to noise ratio.

The data was acquired for 50 replicates using a custom MATLAB program (Mathworks, Natick, MA). A Fast Fourier Transform (FFT) was performed on the signals after the acquisition. The signal intensity was evaluated as an enhancement over control (signal without exosomes) to eliminate the effect of the scattering from the chamber. The linear scattering of the exosomes was assessed at fundamental (5 MHz) component. For nonlinear behavior, the subharmonic (2.25 MHz) and second harmonic (10 MHz) signal enhancements were investigated. The acoustic response of the exosomes was evaluated across four batches of exosomes for ensuring repeatability across batches. To assess the stability of the exosomes under constant ultrasound exposure, the enhancement was monitored for 180 seconds. The experiment was run and compared in sequence with polymersomes of the same concentration for comparison.

2.8 Mannitol concentration variation in preparation protocol

To investigate the role of mannitol[51] in the echogenicity, exosomes were prepared following the same protocol but with varying amounts of mannitol in the HEPES buffer—50, 100, 150, 200, 250, 300, 320, 350 and 400 mM. Evaporation, sonication, and freeze–thaw cycles and freeze-drying were performed as before.

2.9 Injection into the synovial fluid in Sprague Dawley rats

Echogenic exosomes were injected into the synovial fluid of euthanized Sprague Dawley rats. The exosomes were resuspended from powder in BSA–HEPES buffer for a concentration of 58 mg mL^{-1}. Then 100 μL of the solutions was injected into the synovial space. The injections were completed on 4 different knees in 2 different rats. The Vevo 3100 imaging system was used with 40 MHz frequency transducer head. Since the synovial space in rats is small, the area of interested was easy to locate in before and after injection of the exosomes.

2.10 Tail vein injection into NOD Scid Gamma mouse (NSG) mice

Echogenic exosomes were injected into the tail vein of an NSG mouse (IACUC Protocol Number #A18037). The exosomes were resuspended from powder in BSA–HEPES buffer for a concentration of 150 mg mL^{-1}. A 100 μL bolus was injected into the tail vein 3 different times. The Vevo 3100 imaging system was used with a 40 MHz iPixel quantification. The transducer head was fixed throughout the protocol to insure the area being imaged remained constant.

In an ultrasound image obtained by the scanner, areas of interest were selected, maintaining approximately the same area throughout the images. Histograms were created of the pixel counts in the images. Counts were compared to control images and normalized by the area. Analysis of ultrasound images was done using the Fuji image processing package.[52]

3. Results

3.1 Echogenicity

In this article, we assessed the echogenicity of the specially prepared exosomes using three different imaging techniques. Using the Vevo 3100 Imaging System, we imaged the echogenic exosomes in a BSA–HEPES buffer and compared it to the control image of only the BSA–HEPES buffer (Fig. 2). The average brightness of the image was used to evaluate the echogenicity of the particles. In the 4–15 MHz image, the average brightness was 23.1% brighter with exosomes (Fig. 2B) compared to the control (Fig. 2A). The corresponding increase at 21 MHz (Fig. 2C

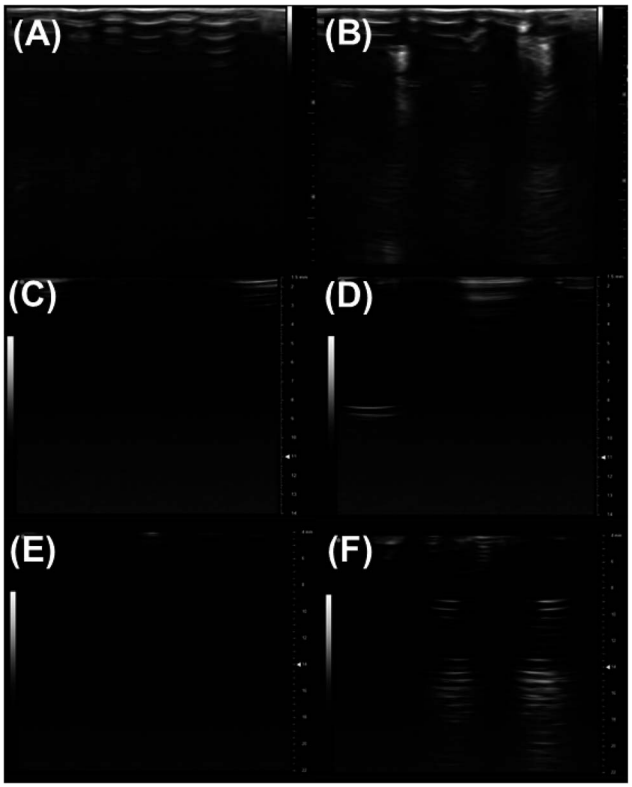

Fig. 2 Ultrasound images of echogenic exosomes in a black 96 well plate, with 250 μL of 5 mg mL^{-1} echogenic exosomes placed in the plate and read with different transducer heads. Images with 4–15 MHz transducer (100% power, 22 fps, 51 dB gain, 60 dB dynamic range) at a depth of 3 cm: (A) BSA–HEPES control and (B) echogenic exosomes. Images with 40 MHz transducers (100% power, 65 fps frame rate, 24 dB gain, depth 10 mm and width 12 mm, 70 dB dynamic range): (C) BSA–HEPES control and (D) echogenic exosomes. Images with 21 MHz transducers (100% power, 34 fps frame rate, 21 dB gain, depth 22 mm and width 21 mm, 60 dB dynamic range for both images): (E) BSA–HEPES control and (F) echogenic exosomes. Brightness and contrast for all images were at 50.

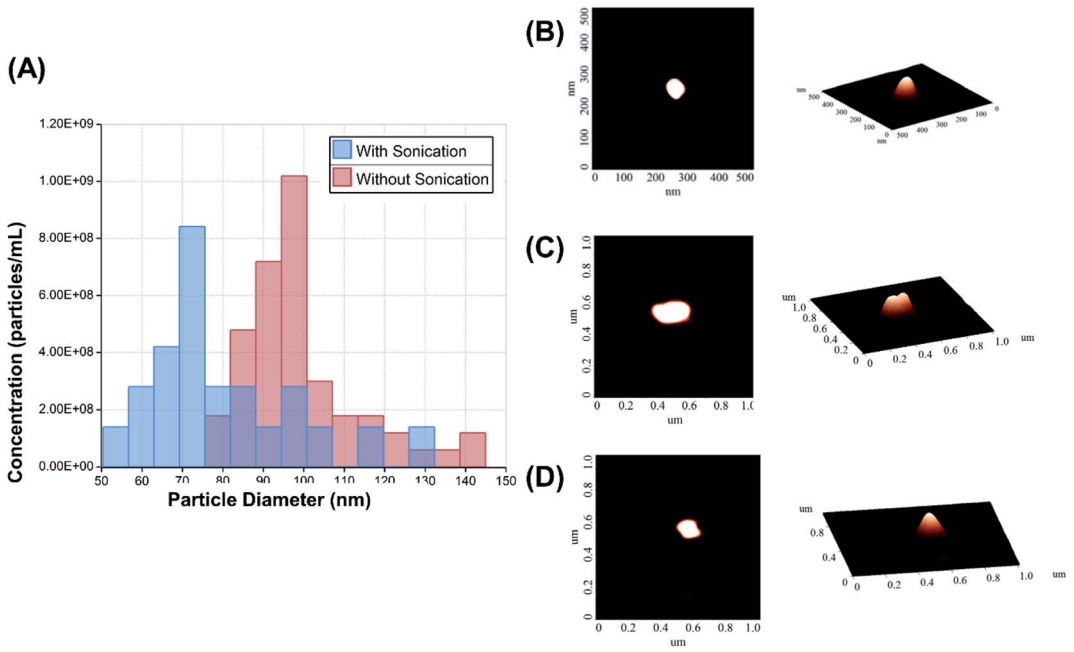

Fig. 3 (A) The size distribution of the echogenic exosomes as measured by the qNano (with and without sonication). Atomic force microscopy images (B–D) of echogenic exosomes. These exosomes range between 60 to 90 nm in diameter after they undergo the protocol to make them echogenic.

Table 1 The average size of exosomes with and without sonication as measured by DLS, AFM, and qNano. PDI is polydispersity index of exosomes

	DLS	PDI of DLS	AFM	qNano
With sonication	101 ± 14 nm	0.43 ± 0.143	60 ± 20 nm	95 ± 26 nm
Without sonication	126 ± 14 nm	0.50 ± 0.13	55 ± 15 nm	107 ± 17 nm

and D) and 40 MHz (Fig. 2E and F) were more than 800% and 28.9% respectively.

3.2 Size morphology and concentration

The size distribution was measured by qNano using a tunable resistive pulse sensing principle (Fig. 3A). AFM images of the echogenic exosomes can be seen in Fig. 3(B) to (D) indicating as expected an approximately spherical morphology. A summary of the average sizes measured by different methods can be seen in Table 1. The average size of the exosomes was found to be 101 ± 14 nm (DLS) and 96 ± 26 nm (qNano) when the solution was sonicated during the preparation. In absence of sonication, the exosomes were slightly larger, with an average diameter of 126 ± 14 nm (DLS) and 107 ± 17 nm (qNano). The concentration of the dry powder was measured to be $4.1 \pm 1.8 \times 10^9$ particles per mg when reconstituted at a concentration of 1 mg mL^{-1}.

3.3 Western blot of exosomes

Western blot analysis of exosomes indicated positive for markers for CD63 and CD9 (Fig. 4) ascertaining that the nanovesicles isolated from bovine milk are indeed exosomes.

3.4 Preparation and reconstitution protocol optimization

The echogenicity of specially prepared echogenic exosomes reconstituted in four different media—PBS, HEPES, BSA, and HEPES–BSA—and with and without sonication during preparation was investigated. In the presence of BSA, we found noticeable effects of echogenic exosomes. We investigated effects of different media and sonication during preparation on exosome echogenicity by directly measuring scattered response in a customized *in*

Fig. 4 Western blot analysis of CD63 and CD9.

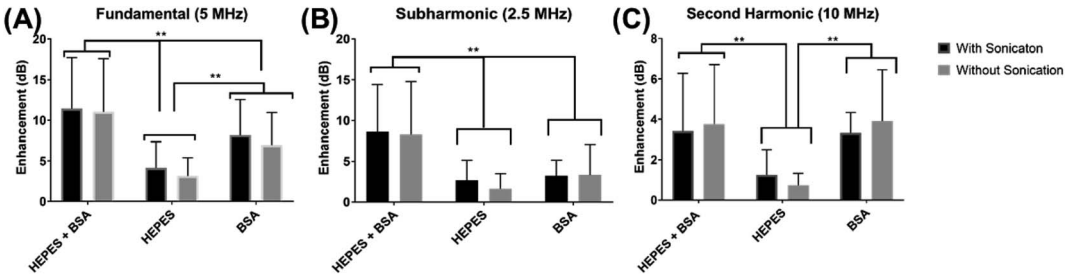

Fig. 5 Scattered enhancements of the echogenic exosome (prepared with and without sonication) solutions for 3 different reconstitution solutions (HEPES + BSA, HEPES, BSA) when exposed to 5 MHz excitation frequencies. Enhancements when compared to control (DI Water) in (A) fundamental, (B) subharmonic and (C) second harmonic. (**$p < 0.001$) (500 kPa pressure amplitude, PRF 100 Hz, 32 cycles).

vitro setup. Both linear and nonlinear scattered signals were recorded when exosomes were exposed to a 5 MHz ultrasound excitation. The enhancement of the scattered fundamental response was highest when the exosomes were reconstituted in 10 mM HEPES + 0.5% BSA—11.4 ± 6.3 dB with sonication during preparation and 11.04 ± 6.6 dB without sonication (Fig. 5A). The signals were significantly higher than when the powder was reconstituted in either 10 mM HEPES or 0.5% BSA by themselves ($p < 0.0001$). When the powder was reconstituted in only 0.5% BSA, the enhancement was also statistically higher than in 10 mM HEPES alone ($p < 0.001$) reaching 8.6 ± 4.4 dB with sonication and 6.8 ± 4.1 dB without sonication. For all solutions, and as we will see below for both linear and nonlinear scattering, there was no significant difference in enhancement with and without sonication during preparation.

Similar to the fundamental response, the enhancement in subharmonic response shown in Fig. 5B was also the highest when the exosomes were reconstituted with 10 mM HEPES + 0.5% BSA ($p < 0.001$). The subharmonic enhancement reached 8.6 ± 6.6 dB with sonication and 8.3 ± 5.8 dB without sonication when reconstituted with 10 mM HEPES + 0.5% BSA. There was no statistical difference between the scattered subharmonic responses when the powder was reconstituted in 10 mM HEPES or 0.5% BSA by themselves.

The second harmonic signal enhancement is shown in Fig. 5C. The scattered signal was similar ($p = 0.9959$) when the

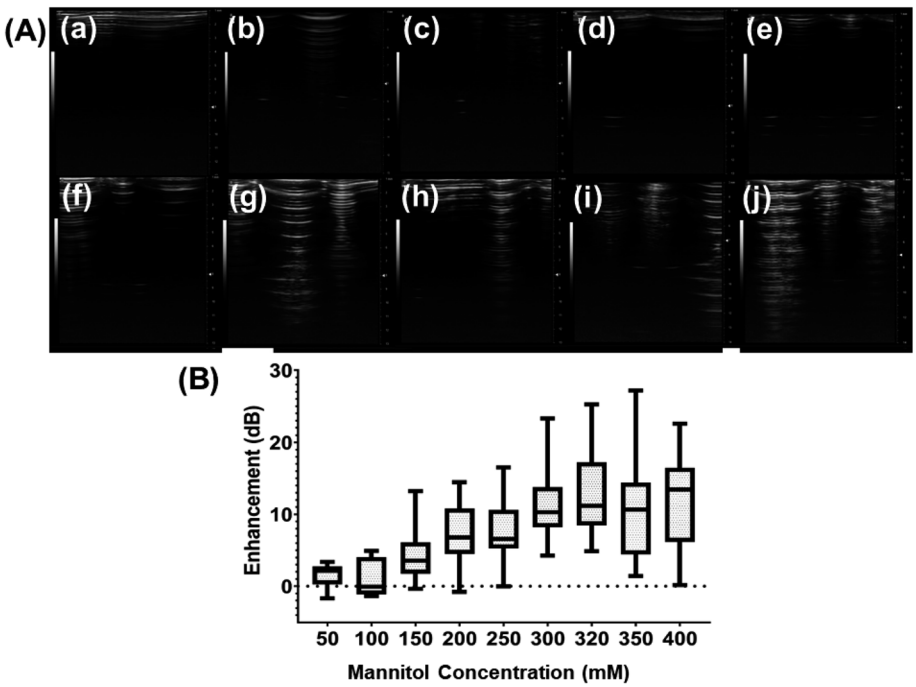

Fig. 6 (A) 40 MHz ultrasound images of echogenic exosomes varying concentrations of mannitol during preparation. (a) Only BSA–HEPES (control), (b) 50 mM, (c) 100 mM, (d) 150 mM, (e) 200 mM, (f) 250 mM, (g) 300 mM, (h) 320 mM, (i) 350 mM, and (j) 400 mM of mannitol. Ultrasound setting is the same for all images taken with Vevo 3100 Imaging System (transmitter frequency 40 MHz, power 100%, frame rate 68 fps, 24 bD, 14 mm depth, 12.08 mm width, 65 dB dynamic range, brightness 50 and contrast 50). (B) Enhancement in fundamental response from echogenic exosomes prepared with varying concentration of mannitol during freeze-dry cycles when exposed to 5 MHz excitation (500 kPa pressure amplitude, PRF 100 Hz, 32 cycles).

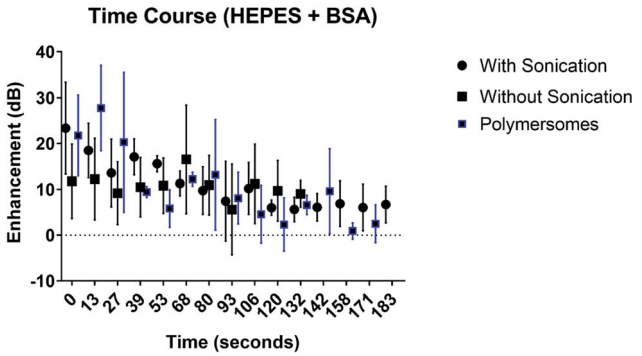

Fig. 7 The fundamental enhancement of the echogenic exosomes (with and without sonication) reconstituted with 10 mM HEPES with 0.5% BSA as compared to echogenic polymersomes of the same concentration over 3 minutes of ultrasound exposure (excitation frequency 5 MHz, 500 kPa pressure amplitude, PRF 100 Hz, 32 cycles).

powder was reconstituted in 10 mM HEPES + 0.5% BSA and 0.5% BSA when the exosomes were reconstituted with 10 mM HEPES + 0.5% BSA, the enhancement of the second harmonic scattered signal was 3.4 ± 2.9 dB with sonication and 3.7 ± 3.0 dB without sonication. The second harmonic scattered signal was 3.3 ± 2.1 dB with sonication and 3.9 ± 2.6 dB without sonication when reconstituted with 0.5% BSA. However, the signal enhancement reduced in the absence of BSA ($p < 0.001$).

3.5 Varying concentration of mannitol

To understand the role that the presence of mannitol during preparation plays in the echogenicity of the exosomes, mannitol concentration was varied. Different batches prepared with different concentrations of mannitol were imaged with the Vevo 3100 Imaging System at 40 MHz (Fig. 6A). There is significant echo when the mannitol concentration rose above 300 mM. We also measure the scattered fundamental response from these batches at 5 MHz (Fig. 6B) using our customized scattering setup. Here also the scattered signal increased as the mannitol concentration increased. Strong backscattered signal was seen only above 150 mM of mannitol.

3.6 Stability under ultrasound

The fundamental signal enhancement due to the echogenic exosomes prepared with or without sonication as well as polymersomes are investigated as a function of time while being exposed to ultrasound excitation (Fig. 7). The enhancement decreased with time. However, the enhancement remains significant even after 3 minutes of exposure similar to what was observed for polymersomes by Xia *et al.*[17] Presence of sonication during preparation didn't change the dynamics.

3.7 *In vivo* imaging of echogenic exosomes

Echogenic exosomes were injected into the synovial space of a Sprague Dawley rat (Fig. 8). Injecting echogenic exosomes (Fig. 8B) results in a brighter image when compared to control (Fig. 8A). It is further validated by the quantification of pixel brightness (Fig. 8C) showing a 37.2% increase in brightness of the images upon the injection of the exosomes. The exosomes were also injected into the tail vein of an NSG mouse (Fig. 9). The images of the mouse kidney were found to be enhanced by the addition of exosomes (Fig. 9B) when compared to before the exosomes were injected (Fig. 9A) as also shown by pixel histogram (Fig. 9C). There was more than 3-fold increase in brightness when the echogenic exosomes were injected into the vein.

4. Discussion

Exosomes are naturally secreted bilayer vesicles known to play critical roles in inter-cellular communications and transport. Utilizing bovine milk exosomes provides unique advantages and has been shown to be effective and non-toxic within *in vitro* and *in vivo* environments. Here they have been isolated from bovine milk and then made to undergo a specialized protocol of repeated freeze-thaw cycles followed by a freeze-drying process in the presence of mannitol that made them echogenic. The procedure was motivated by our as well as others' studies that indicated that mannitol plays a crucial role during the preparation of echogenic liposomes and polymersomes encapsulating gaseous cores that render such vesicles echogenic.[24,51,53] The echogenicity of the specially prepared exosomes were investigated using commercial ultrasound scanner both *in vitro* and *in vivo*. We also measure their scattered responses in a customized setup. This is the first ever report of echogenicity of exosomes offering potentials for their concurrent ultrasound imaging and drug delivery capabilities.

There was a noticeable difference in brightness between the ultrasound scanner images of echogenic exosomes and the

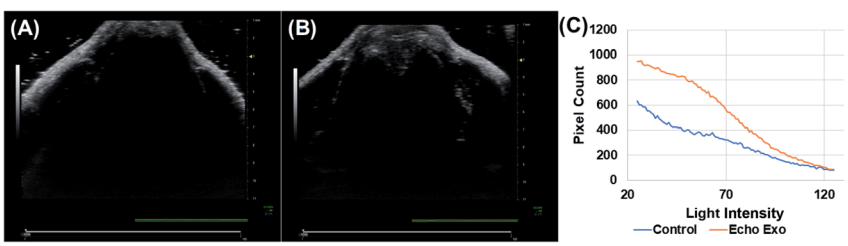

Fig. 8 Ultrasound images (A) before and (B) after injection of echogenic exosomes into the synovial space of a Sprague Dawley rat. Images were taken with a Vevo 3100 Imaging System and 40 MHz transducer head (at 100% power, 76 fps frame rate, 25 dB gain, depth 11.00 mm and width 14.08 mm, 70 dB dynamic range, brightness 50 and contrast 50 for both images). (C) Pixel counts from (A) and (B) echogenic exosomes before (blue) and after (orange) injection into synovial space. Pixel count was normalized by the area for all graphs.

Fig. 9 Ultrasound images of mouse kidney (A) before and (B) after injection of echogenic exosomes (100 μl of 58 mg mL^{-1}) into the tail vein of NSG mouse using Vevo 3100 Imaging System and 40 MHz transducer head (at 100% power, 70 fps frame rate, 25 dB gain, depth 10 mm and width 18 mm, 70 dB dynamic range, brightness 50 and contrast 50 for both images). (C) Pixel count differences of light intensity between echogenic exosomes before (blue) and after (red) tail vein injection. Pixel count was normalized by the area for the graph.

control images at three different frequencies (Fig. 2). The average brightness in all three imaging environments demonstrate that the exosomes became responsive to ultrasound after undergoing the specialized protocol of repeated freeze–thaw and freeze-drying in presence of mannitol.

After the exosomes underwent the preparation protocol, the size and the concentration of exosomes in the resulting powder were quantified using DLS, AFM, and qNano. The measured sizes lie within the expected range of 40–130 nm. The exosomes did not appear to be destroyed through the freeze-drying procedure, and $4.1 \pm 1.8 \times 10^9$ particles per mg were present in the freeze-dried powder. When the particles were measured by AFM, the shapes appeared to have remained roughly spherical with a slightly smaller diameter of roughly 60 nm (Fig. 3). The smaller diameter in AFM observation could have resulted from drying of the sample for AFM imaging. Fig. 3A indicates that with sonication, the size distribution shifts to the left resulting is slightly reduced average size in Table 1. But the similarity in average size with and without sonication indicates very little destruction of exosomes due to sonication. Echogenic exosomes are slightly smaller than echogenic liposomes (125–185 nm)[24] and much smaller than echogenic polymersomes (400–450 nm).[17] The smaller size and natural morphology make echogenic exosomes an ideal candidate for drug delivery without immune responses but with added capabilities due to its responsiveness to ultrasound.[1]

Ultrasound contrast agents are known to generate both linear and nonlinear response to ultrasound excitation.[17,24,37,38,45,54] We investigated the ability of the echogenic exosomes reconstituted in three different media—HEPS, BSA, HEPS + BSA—to generate the linear and nonlinear responses (Fig. 5). Echogenic exosomes show strong sub- and second-harmonic scattered responses. The strong nonlinear responses offer possibilities for their applications in nonlinear imaging modalities with better signal-to-tissue ratios.[55,56] For all reconstitution parameters and at all receiving frequencies, there was no statistical difference between the signal enhancement of exosomes prepared with and without sonication. This could be due to the similarity in size between these echogenic exosomes.

Echogenicity of the exosomes varied with variation in reconstitution media. The linear and nonlinear signal enhancements were statistically higher in cases where BSA was added to the solution compared to being reconstituted in HEPES alone (Fig. 5). This was also borne out by ultrasound scanner images (40 MHz transducer) of exosomes prepared in these three different media (data not shown). The addition of BSA appears to be critical to the scattering behavior of the exosomes. Kumar *et al.* while exploring the role of freeze-dried mannitol on the echogenicity of liposomes and polymersomes also found strong echogenicity of freeze-dried mannitol powder by itself in DI water, which is further enhanced by addition of BSA.[57] It was hypothesized that BSA acts like a surfactant to the microbubbles stabilizing them and allowing them to remain in the solution longer. The present study seems to indicate a similar stabilizing role of BSA for the air pockets created in association with exosomes.

As noted before, mannitol has been assumed to play a critical role in ensuring echogenicity in specially prepared liposomes and polymersomes.[24,53,58–61] We investigated the echogenicity of specially modified exosomes varying amount of mannitol during the freeze-dry process, ranging from 50 to 400 mM. Previously, we have demonstrated that the crystalline nature of mannitol facilitates bubble generation during dissolution,[57] and we believe that mannitol is the key to the echogenicity of the echogenic liposomes, polymersomes, and exosomes. Similar to the findings of Paul *et al.*[24] for echogenic liposomes, ultrasound images of echogenic exosomes freeze dried in the presence of different concentrations of mannitol (Fig. 6A) and their enhancement (Fig. 6B) showed echogenicity when freeze-drying was performed with mannitol at a concentration above 150 mM.

We chose freeze drying in the presence of 320 mM of mannitol and reconstitution in BSA–HEPES with sonication as our preparation protocol of choice. Exosomes thus prepared were investigated for their stability and *in vivo* imaging potential (Fig. 7). The stability of the echogenic exosomes appears to be similar to echogenic polymersomes[53]—echogenic even after 3 minutes of constant ultrasound exposure at a 5 MHz excitation frequency.

To explore their *in vivo* imaging potential, echogenic exosomes were injected in the synovial fluid of Sprague Dawley rats and into the tail vein of NSG mice and imaged at 40 MHz. In both cases, the image pixel brightness clearly showed enhancements after echogenic exosome injection (Fig. 8 and 9).

The enhancements were 37.2% in case of the synovial fluid of the rats and 300% for mice.

Exosomes—specially modified here by a freeze-drying process in presence of mannitol—have demonstrated significant echogenicity in ultrasound scanner as well as in customized *in vitro* scattering setup. Liposomes and polymersomes have previously been shown to be echogenic when prepared by freeze-drying in presence of mannitol. Small air-pockets were hypothesized to be situated in the bilayer, outside or inside such echogenic vesicles.[24,53,58] Recently, Shekhar *et al.* evaluated the nature of the echogenic behaviors of liposomes using differential interference contrast microcopy (DIC).[62] Their DIC images showed micrometer sized bubbles encapsulated inside liposome, but the typical size of the observable liposomes in the DIC images were far larger; the number weighted and volume-weighted diameters of these vesicles were 1.35 μm and 8.23 μm respectively.[62] The exosomes studied here, unlike previously studied echogenic liposomes and the polymersomes, are preformed vesicles, but they underwent the same freeze-drying procedure in presence of mannitol that was also part of the preparation protocol for echogenic liposomes and polymersomes.[18,24,28,53,58,63–65] However, unlike echogenic liposomes carrying encapsulated microbubble inside studied by Shekhar *et al.*[62] the echogenic exosomes are much smaller in size—50–150 nm. The smaller nanometer size of the exosomes indicates similarity to nanocups and other such nanoparticles investigated by Kwan *et al.*[66] which spontaneously grow surface trapped bubbles upon ultrasound excitation due to their geometry and surface properties. However, further investigation is needed for elucidating the origin of the echogenicity of these nanoparticles.

While the exact location of the bubble remains uncertain for the application of the exosomes, the results here also imply that the presence of mannitol during the freeze-drying process and reconstituting the freeze-dried powder in solutions containing BSA are critical for creating and maintaining echogenic behavior or the exosomes.[62,66] These results indicate that echogenic exosomes, when prepared following the specialized protocol described here, hold promising potential for use in contrast ultrasound imaging as well as drug delivery application when loaded with appropriate drugs.

5. Conclusion

Exosomes are naturally secreted nanoparticles—diameters 40–130 nm—that inherit the morphology and contain the biological information of the parent cell. Their structure and size make them ideal for potential drug delivery applications. Here for the first time, we proposed and demonstrated a procedure for rendering bovine milk-derived exosomes echogenic. The exosomes, that underwent the specialized protocol, were shown to be echogenic through an array of *in vitro* and *in vivo* investigation using a commercial ultrasound scanner as well as a customized setup. The acoustic behavior was found to be similar to that of echogenic liposomes or polymersomes. Previously, exosomes have shown success in being able to be functionalized and loaded with a variety of drugs.[2] The ability to make them echogenic, along with the large scale extractability from bovine milk, opens the possibility for their applications as ultrasound contrast agents or as ultrasound responsive drug delivery vehicles.

Author contributions

JO and JP contributed to experimental design, performed experiments, and wrote the manuscript. SM and KS contributed to experimental design and writing the manuscript. JF, JS, KG, TM, YC, and AB assisted in performing experiments.

Ethical statement

All mice were housed under standard housing conditions at the Animal Studies Core Facility of North Dakota State University (NDSU). All animal procedures were reviewed and approved by the Institute of Animal Care and Use Committee at the NDSU, protocol number 17052.

Conflicts of interest

There are no conflicts to declare.

Acknowledgements

This research was supported by NIH grant 1 R01GM 114080 to S.M. and K.S. JO and KS would like to acknowledge the ARCS MWC Chapter, The McNichols Family Foundation, and The Myers family for their support.

References

1 M. S. Kim, M. J. Haney, Y. Zhao, V. Mahajan, I. Deygen, N. L. Klyachko, E. Inskoe, A. Piroyan, M. Sokolsky, O. Okolie, S. D. Hingtgen, A. V. Kabanov and E. V. Batrakova, Development of Exosome-encapsulated Paclitaxel to Overcome MDR in Cancer cells, *Nanomedicine*, 2016, **12**(3), 655–664.

2 A. V. Vlassov, S. Magdaleno, R. Setterquist and R. Conrad, Exosomes: Current knowledge of their composition, biological functions, and diagnostic and therapeutic potentials, *Biochim. Biophys. Acta, Gen. Subj.*, 2012, **1820**(7), 940–948.

3 J. E. Pullan, M. I. Confeld, J. K. Osborn, J. Kim, K. Sarkar and S. Mallik, Exosomes as Drug Carriers for Cancer Therapy, *Mol. Pharm.*, 2019, **16**(5), 1789–1798.

4 A. Makler and W. Asghar, Exosomal biomarkers for cancer diagnosis and patient monitoring, *Expert Rev. Mol. Diagn.*, 2020, 1–14.

5 Z. Sun, L. Wang, S. Wu, Y. Pan, Y. Dong, S. Zhu, J. Yang, Y. Yin and G. Li, An Electrochemical Biosensor Designed by Using Zr-Based Metal–Organic Frameworks for the Detection of Glioblastoma-Derived Exosomes with Practical Application, *Anal. Chem.*, 2020, **92**, 3819–3826.

6 M. S. Chiriaco, M. Bianco, A. Nigro, E. Primiceri, F. Ferrara, A. Romano, A. Quattrini, R. Furlan, V. Arima and

G. Maruccio, Lab-on-Chip for Exosomes and Microvesicles Detection and Characterization, *Sensors*, 2018, **18**(10), 3175.
7 A. Kumari, S. K. Yadav and S. C. Yadav, Biodegradable polymeric nanoparticles based drug delivery systems, *Colloids Surf., B*, 2010, **75**(1), 1–18.
8 M. Kundranda and J. Niu, Albumin-bound paclitaxel in solid tumors: clinical development and future directions, *Drug Des., Dev. Ther.*, 2015, 3767.
9 J. W. Shreffler, J. E. Pullan, K. M. Dailey, S. Mallik and A. E. Brooks, Overcoming Hurdles in Nanoparticle Clinical Translation: The Influence of Experimental Design and Surface Modification, *Int. J. Mol. Sci.*, 2019, **20**(23), 6056.
10 K. Cho, X. Wang, S. Nie, Z. Chen and D. M. Shin, Therapeutic Nanoparticles for Drug Delivery in Cancer, *Clin. Cancer Res.*, 2008, **14**(5), 1310–1316.
11 Y. Tian, S. Li, J. Song, T. Ji, M. Zhu, G. J. Anderson, J. Wei and G. Nie, A doxorubicin delivery platform using engineered natural membrane vesicle exosomes for targeted tumor therapy, *Biomaterials*, 2014, **35**(7), 2383–2390.
12 M. P. di Magliano and C. D. Logsdon, Roles for KRAS in pancreatic tumor development and progression, *Gastroenterology*, 2013, **144**(6), 1220–1229.
13 Y. Yang, D. Pan, K. Luo, L. Li and Z. Gu, Biodegradable and amphiphilic block copolymer-doxorubicin conjugate as polymeric nanoscale drug delivery vehicle for breast cancer therapy, *Biomaterials*, 2013, **34**(33), 8430–8443.
14 F. Aqil, R. Munagala, J. Jeyabalan, A. K. Agrawal and R. Gupta, Exosomes for the Enhanced Tissue Bioavailability and Efficacy of Curcumin, *AAPS J.*, 2017, **19**(6), 1691–1702.
15 C. Théry, L. Zitvogel and S. Amigorena, Exosomes: composition, biogenesis and function, *Nat. Rev. Immunol.*, 2002, **2**(8), 569–579.
16 J. Pan, M. Ding, K. Xu, C. Yang and L.-J. Mao, Exosomes in diagnosis and therapy of prostate cancer, *Oncotarget*, 2017, **8**(57), 97693–97700.
17 L. Xia, F. Karandish, K. N. Kumar, J. Froberg, P. Kulkarni, K. N. Gange, Y. Choi, S. Mallik and K. Sarkar, Acoustic Characterization of Echogenic Polymersomes Prepared From Amphiphilic Block Copolymers, *Ultrasound Med. Biol.*, 2018, **44**(2), 447–457.
18 R. Nahire, M. K. Haldar, S. Paul, A. Mergoum, A. H. Ambre, K. S. Katti, K. N. Gange, D. K. Srivastava, K. Sarkar and S. Mallik, Polymer-Coated Echogenic Lipid Nanoparticles with Dual Release Triggers, *Biomacromolecules*, 2013, **14**(3), 841–853.
19 P. Kulkarni, M. K. Haldar, S. You, Y. Choi and S. Mallik, Hypoxia-Responsive Polymersomes for Drug Delivery to Hypoxic Pancreatic Cancer Cells, *Biomacromolecules*, 2016, **17**(8), 2507–2513.
20 T. Anajafi, M. D. Scott, S. You, X. Yang, Y. Choi, S. Y. Qian and S. Mallik, Acridine Orange Conjugated Polymersomes for Simultaneous Nuclear Delivery of Gemcitabine and Doxorubicin to Pancreatic Cancer Cells, *Bioconjugate Chem.*, 2016, **27**(3), 762–771.
21 T. Anajafi and S. Mallik, Polymersome-based drug-delivery strategies for cancer therapeutics, *Ther. Delivery*, 2015, **6**(4), 521–534.
22 J. C. Kraft, J. P. Freeling, Z. Wang and R. J. Y. Ho, Emerging Research and Clinical Development Trends of Liposome and Lipid Nanoparticle Drug Delivery Systems, *J. Pharm. Sci.*, 2014, **103**(1), 29–52.
23 E. J. Bunggulawa, W. Wang, T. Yin, N. Wang, C. Durkan, Y. Wang and G. Wang, Recent advancements in the use of exosomes as drug delivery systems, *J. Nanobiotechnol.*, 2018, **16**(1), 81.
24 S. Paul, D. Russakow, R. Nahire, T. Nandy, A. H. Ambre, K. Katti, S. Mallik and K. Sarkar, In vitro measurement of attenuation and nonlinear scattering from echogenic liposomes, *Ultrasonics*, 2012, **52**(7), 962–969.
25 J. A. Kopechek, T. M. Abruzzo, B. Wang, S. M. Chrzanowski, D. A. B. Smith, P. H. Kee, S. Huang, J. H. Collier, D. D. McPherson and C. K. Holland, Ultrasound-Mediated Release of Hydrophilic and Lipophilic Agents From Echogenic Liposomes, *J. Ultrasound Med.*, 2008, **27**(11), 1597–1606.
26 J. A. Kopechek, K. J. Haworth, J. L. Raymond, T. Douglas Mast, S. R. Perrin, M. E. Klegerman, S. Huang, T. M. Porter, D. D. McPherson and C. K. Holland, Acoustic characterization of echogenic liposomes: Frequency-dependent attenuation and backscatter, *J. Acoust. Soc. Am.*, 2011, **130**(5), 3472–3481.
27 H. Alkan-Onyuksel, S. M. Demos, G. M. Lanza, M. J. Vonesh, M. E. Klegerman, B. J. Kane, J. Kuszak and D. D. McPherson, Development of Inherently Echogenic Liposomes as an Ultrasonic Contrast Agent†, *J. Pharm. Sci.*, 1996, **85**(5), 486–490.
28 S. Paul, R. Nahire, S. Mallik and K. Sarkar, Encapsulated microbubbles and echogenic liposomes for contrast ultrasound imaging and targeted drug delivery, *Comput. Mech.*, 2014, **53**(3), 413–435.
29 B. B. Goldberg; J. S. Raichlen and F. Forsberg, *Ultrasound Contrast Agents: Basic Principles and Clinical Applications*, Martin Dunitz, London, 2nd edn, 2001, p. 440.
30 N. deJong, F. J. Tencate, C. T. Lancee, J. R. T. C. Roelandt and N. Bom, Principles and Recent Developments in Ultrasound Contrast Agents, *Ultrasonics*, 1991, **29**(4), 324–330.
31 R. Bekeredjian, P. A. Grayburn and R. V. Shohet, Use of ultrasound contrast agents for gene or drug delivery in cardiovascular medicine, *J. Am. Coll. Cardiol.*, 2005, **45**(3), 329–335.
32 V. Paefgen, D. Doleschel and F. Kiessling, Evolution of contrast agents for ultrasound imaging and ultrasound-mediated drug delivery, *Front. Pharmacol.*, 2015, **6**, 197.
33 I. Durot, S. R. Wilson and J. K. Willmann, Contrast-enhanced ultrasound of malignant liver lesions, *Abdominal Radiology*, 2018, **43**(4), 819–847.
34 K. Sarkar, A. Katiyar and P. Jain, Growth and dissolution of an encapsulated contrast microbubble, *Ultrasound Med. Biol.*, 2009, **35**(8), 1385–1396.

35 A. Katiyar, K. Sarkar and P. Jain, Effects of Encapsulation Elasticity on the stability of an Encapsulated Microbubble, *J. Colloid Interface Sci.*, 2009, **336**, 519–525.
36 A. Katiyar and K. Sarkar, Stability analysis of an encapsulated microbubble against gas diffusion, *J. Colloid Interface Sci.*, 2010, **343**(1), 42–47.
37 D. Chatterjee and K. Sarkar, A Newtonian rheological model for the interface of microbubble contrast agents, *Ultrasound Med. Biol.*, 2003, **29**(12), 1749–1757.
38 K. Sarkar, W. T. Shi, D. Chatterjee and F. Forsberg, Characterization of ultrasound contrast microbubbles using in vitro experiments and viscous and viscoelastic interface models for encapsulation, *J. Acoust. Soc. Am.*, 2005, **118**(1), 539–550.
39 S. Paul, A. Katiyar, K. Sarkar, D. Chatterjee, W. T. Shi and F. Forsberg, Material characterization of the encapsulation of an ultrasound contrast microbubble and its subharmonic response: Strain-softening interfacial elasticity model, *J. Acoust. Soc. Am.*, 2010, **127**(6), 3846–3857.
40 S. Paul, D. Russakow, T. Rodgers, K. Sarkar, M. Cochran and M. A. Wheatley, Determination of the interfacial rheological properties of a Poly(DL-lactic acid)-encapsulated contrast agent uning in vitro attenuation and scattering, *Ultrasound Med. Biol.*, 2013, **39**(7), 1277–1291.
41 K. N. Kumar and K. Sarkar, Interfacial Rheological Properties of Contrast Microbubble Targestar P as a Function of Ambient Pressure, *Ultrasound Med. Biol.*, 2016, **42**(4), 1010–1017.
42 N. Mobadersany and K. Sarkar, Acoustic microstreaming near a plane wall due to a pulsating free or coated bubble: velocity, vorticity and closed streamlines, *J. Fluid Mech.*, 2019, **875**, 781–806.
43 E. Stride and N. Saffari, Microbubble ultrasound contrast agents: A review, *Proc. Inst. Mech. Eng., Part H*, 2003, **217**(6), 429–447.
44 J. Osborn, M. Aliabouzar, X. Zhou, R. Rao, L. G. Zhang and K. Sarkar, Enhanced Osteogenic Differentiation of Human Mesenchymal Stem Cells Using Microbubbles and Low Intensity Pulsed Ultrasound on 3D Printed Scaffolds, *Adv. Biosyst.*, 2019, **3**(2), 1800257.
45 M. Aliabouzar, K. N. Kumar and K. Sarkar, Acoustic vaporization threshold of lipid-coated perfluoropentane droplets, *J. Acoust. Soc. Am.*, 2018, **143**(4), 2001–2012.
46 M. Aliabouzar, K. N. Kumar and K. Sarkar, Effects of droplet size and perfluorocarbon boiling point on the frequency dependence of acoustic vaporization threshold, *J. Acoust. Soc. Am.*, 2019, **145**(2), 1105–1116.
47 R. Munagala, F. Aqil, J. Jeyabalan and R. C. Gupta, Bovine milk-derived exosomes for drug delivery, *Cancer Lett.*, 2016, **371**(1), 48–61.
48 M. Somiya, Y. Yoshioka and T. Ochiya, Biocompatibility of highly purified bovine milk-derived extracellular vesicles, *J. Extracell. Vesicles*, 2018, **7**(1), 1440132.
49 F. Karandish, B. Mamnoon, L. Feng, M. K. Haldar, L. Xia, K. N. Gange, S. You, Y. Choi, K. Sarkar and S. Mallik, Nucleus-Targeted, Echogenic Polymersomes for Delivering a Cancer Stemness Inhibitor to Pancreatic Cancer Cells, *Biomacromolecules*, 2018, **19**(10), 4122–4132.
50 S. Paul, D. Russakow, T. Rodgers, K. Sarkar, M. Cochran and M. A. Wheatley, Determination of the Interfacial Rheological Properties of a Poly(DL-lactic acid)-Encapsulated Contrast Agent Using In Vitro Attenuation and Scattering, *Ultrasound Med. Biol.*, 2013, **39**(7), 1277–1291.
51 K. N. Kumar, S. Mallik and K. Sarkar, Role of freeze-drying in the presence of mannitol on the echogenicity of echogenic liposomes, *J. Acoust. Soc. Am.*, 2017, **142**(6), 3670–3676.
52 J. Schindelin, I. Arganda-Carreras, E. Frise, V. Kaynig, M. Longair, T. Pietzsch, S. Preibisch, C. Rueden, S. Saalfeld, B. Schmid, J.-Y. Tinevez, D. J. White, V. Hartenstein, K. Eliceiri, P. Tomancak and A. Cardona, Fiji: an open-source platform for biological-image analysis, *Nat. Methods*, 2012, **9**, 676.
53 L. Xia, F. Karandish, K. N. Kumar, J. Froberg, P. Kulkarni, K. N. Gange, Y. Choi, S. Mallik and K. Sarkar, Acoustic Characterization Of Echogenic Polymersomes Prepared From Amphiphilic Block Copolymers, *Ultrasound Med. Biol.*, 2018, **44**(2), 447–457.
54 K. N. Kumar and K. Sarkar, Effects of ambient hydrostatic pressure on the material properties of the encapsulation of an ultrasound contrast microbubble, *J. Acoust. Soc. Am.*, 2015, **138**(2), 624–634.
55 A. Katiyar, K. Sarkar and F. Forsberg, Modeling subharmonic response from contrast microbubbles as a function of ambient static pressure, *J. Acoust. Soc. Am.*, 2011, **129**(4), 2325–2335.
56 F. Forsberg, W. T. Shi and B. B. Goldberg, Subharmonic imaging of contrast agents, *Ultrasonics*, 2000, **38**(1–8), 93–98.
57 K. N. Kumar, S. Mallik and K. Sarkar, Role of freeze-drying in the presence of mannitol on the echogenicity of echogenic liposomes, *J. Acoust. Soc. Am.*, 2017, **142**(6), 3670–3676.
58 S. L. Huang, A. J. Hamilton, A. Nagaraj, S. D. Tiukinhoy, M. E. Klegerman, D. D. McPherson and R. C. MacDonald, Improving ultrasound reflectivity and stability of echogenic liposomal dispersions for use as targeted ultrasound contrast agents, *J. Pharm. Sci.*, 2001, **90**(12), 1917–1926.
59 S. L. Huang, A. J. Hamilton, E. Pozharski, A. Nagaraj, M. E. Klegerman, D. D. McPherson and R. C. MacDonald, Physical correlates of the ultrasonic reflectivity of lipid dispersions suitable as diagnostic contrast agents, *Ultrasound Med. Biol.*, 2002, **28**(3), 339–348.
60 S. L. Huang and R. C. MacDonald, Acoustically active liposomes for drug encapsulation and ultrasound-triggered release, *Biochim. Biophys. Acta, Biomembr.*, 2004, **1665**(1–2), 134–141.
61 J. A. Kopechek, K. J. Haworth, J. L. Raymond, T. Douglas Mast, S. R. Perrin Jr, M. E. Klegerman, S. Huang, T. M. Porter, D. D. McPherson and C. K. Holland, Acoustic characterization of echogenic liposomes: Frequency-dependent attenuation and backscatter, *J. Acoust. Soc. Am.*, 2011, **130**(5), 3472–3481.
62 H. Shekhar, R. T. Kleven, T. Peng, A. Palaniappan, K. B. Karani, S. Huang, D. D. McPherson and C. K. Holland, In vitro characterization of

sonothrombolysis and echocontrast agents to treat ischemic stroke, *Sci. Rep.*, 2019, **9**(1), 9902.

63 R. Nahire, S. Paul, M. D. Scott, R. K. Singh, W. W. Muhonen, J. Shabb, K. N. Gange, D. K. Srivastava, K. Sarkar and S. Mallik, Ultrasound Enhanced Matrix Metalloproteinase-9 Triggered Release of Contents from Echogenic Liposomes, *Mol. Pharm.*, 2012, **9**(9), 2554–2564.

64 R. Nahire, R. Hossain, R. Patel, S. Paul, V. Meghnani, A. H. Ambre, K. N. Gange, K. S. Katti, E. Leclerc, D. K. Srivastava, K. Sarkar and S. Mallik, pH-Triggered Echogenicity and Contents Release from Liposomes, *Mol. Pharm.*, 2014, **11**(11), 4059–4068.

65 R. Nahire, M. K. Haldar, S. Paul, A. H. Ambre, V. Meghnani, B. Layek, K. S. Katti, K. N. Gange, J. Singh, K. Sarkar and S. Mallik, Multifunctional polymersomes for cytosolic delivery of gemcitabine and doxorubicin to cancer cells, *Biomaterials*, 2014, **35**(24), 6482–6497.

66 J. J. Kwan, R. Myers, C. M. Coviello, S. M. Graham, A. R. Shah, E. Stride, R. C. Carlisle and C. C. Coussios, Ultrasound-Propelled Nanocups for Drug Delivery, *Small*, 2015, **11**(39), 5305–5314.

